LBL-5239

FIZIKA 9 (1977) Supplement 4, 623–670

(Proceedings of the Int. Symp. on Nuclear Collisions and Their Microscopic Description, Bled, September 1977)

COMPARISON OF MODELS OF HIGH ENERGY HEAVY ION COLLISION*

Miklos Gyulassy
Nuclear Science Division
Lawrence Berkeley Laboratory
University of California
Berkeley, California 94720 USA

ABSTRACT: Some of the main theoretical developments on heavy ion collisions at energies (0.1 ~ 2.0) GeV/nuc are reviewed. The fireball, firestreak, hydrodynamic (1-fluid, 2-fluids), "row on row", hard sphere and intranuclear cascades, and classical equations of motion models are discussed in detail. Results are compared to each other and to measured Ne + U → p + X reactions.

The report contains: I. Introduction (Expectations, hopes and goals; Obstacles), II. Choice of theoretical framework (The ultimate and less; Classical Methods; The need for variaty of models), III. The zoo of models (The fireball; Firestraak; Hydrodynamics; Row on row; Hard spheres; Cascade 1; Cascade 2; Comparison of results), IV. Summary and outlook.

I. INTRODUCTION

In the past few years the field of high energy (100 MeV - 2 GeV per nucleon) heavy ion collisions has expanded rapidly, both experimentally and theoretically. There is now a wealth of data[1] at these energies on single particle inclusive cross sections, $d^2\sigma(P+T\to F+X)/d\Omega_F dE_F$, for a variety of projectiles P = p,d,α,C,Ne,Ar, and targets T = C, Na,Cu,Ar,Pb,U, and fragments F = $\pi^{\pm}$,p,d,t,α,.... Semi-inclusive and exclusive processes are also currently being measured. During this time a variety of theoretical models of heavy ion dynamics have also emerged. The purpose of this report is to review some of the major theoretical developments to date.[2]

I.1 Expectations, hopes, and goals

To begin the discussion, we recall first the main expectations, hopes, and goals of high energy heavy ion physics. In particular, what new physical domains can we expect the field to cover? What novel phenomena can we hope to observe? Finally, what are the goals as to the new physics we want to extract from heavy ion collisions?

At energies E > 100 MeV/nucleon, the relative nucleon velocities exceed typical sound velocities, $\lesssim c/3$, in nuclear matter, and, hence, density pile-ups are expected to occur. Even in the absence of interactions simple interpenetration would lead to double densities, $\rho = 2\rho_o$, $\rho_o = 0.17$ fm^{-3}. With interactions, much higher densities $\rho \gtrsim 4\,\rho_o$ can be reached in strong shock zones. However, such high densities can be attained only at the price of high excitation energies, $E^* \sim$ 50-100 MeV/nucleon. Thus, we expect extreme conditions

during heavy ion collisions with $\rho > \rho_o$ and $E^* > E_F$ = Fermi energy, that are far outside the realm of conventional nuclear physics ($\rho \leq \rho_o$, $E^* << E_F$).

The hope is that novel states of nuclear matter or unusual collective phenomena will manifest themselves under those extreme conditions. As the density increases, more nucleons come within the range of each others' forces. Long range correlations can then develop resulting in phase transitions in nuclear matter. Model calculations in fact suggest that such phase transitions are likely to occur for $\rho \gtrsim 2\rho_o$. In particular, phase transitions leading to density isomers[3] and pion condensates[4] have been extensively studied. Speculations[5] have also arisen suggesting that at high ρ, nucleons would lose their identity and merge into a new state of quark matter. The hope then in heavy ion physics is that some such exotic phenomena could be observed.

However, whether exotic phenomena occur or not, an immediate goal of heavy ion physics is to learn about the nuclear equation of state: $W(\rho,T)$ = energy per nucleon as a function of density and temperature. Incredibly, the only thing known about W today is that $W(\rho_o,0) = -16$ MeV and $\partial W/\partial\rho = 0$ at $(\rho_o,0)$. Even the incompressibility $K = 9\rho_o^2\partial^2 W/\partial\rho^2$ at $(\rho_o,0)$ is unknown - estimates range, from ~150 - 400 MeV. The determination of K alone would constitute a great achievement of heavy ion physics. The determination of $W(\rho,T)$ over any finite region of the (ρ,T) plane would thus vastly expand our understanding of nuclear physics.

I.2 Obstacles

There may, however, be major obstacles in the way of determining $W(\rho,T)$ from heavy ion collisions. The most significant one is that only asymptotic states can be observed experimentally. While the actual dynamical path in such collisions may depend on $W(\rho,T)$ over a wide range of ρ and T, only the final stage of the dynamics is observed. In particular, there may be many different $W(\rho,T)$ that lead to the same final energy and angle distributions. Another obstacle is that $W(\rho,T)$ makes sense only if local equilibrium is reached during the collision. Otherwise, we would observe only transient properties of the system as it evolves from the initial highly non-equilibrium configuration toward equilibrium. Finally, heavy ion collisions involve finite systems where surface effects (curvature, diffuseness), not described by $W(\rho,T)$, could be important. Thus, for example, sharp Mach cones[6] developed in central shock regions could be considerably smeared out by refraction through the curved surfaces. Clearly, only model calculations can assess the real importance of the above obstacle.

II. CHOICE OF THEORETICAL FRAMEWORK

Before discussing the specific models though, we consider the question of which theoretical framework is expected to be appropriate for high energy heavy ion collisions. This discussion is tailored after Refs. [7,8].

II.1 The Ultimate and Less

The important aspects of heavy ion dynamics that should be incorporated in some way are (1) particle (π) production, (2) relativistic kinematics, (3) interactions between nucleons: binding and correlations (e.g., d,α,..., clustering), (4) quantum interference and coherence effects: virtual fluctuations, off-shell effects, and (5) finite geometry.

The most general framework that includes all the above aspects is Relativistic Quantum Field Theory with meson degrees of freedom treated explicitly. However, this "Nirvana"[8] is as yet unattainable by mere mortals. So we are forced to settle for less and consider simplifications and idealizations.

Since particle production greatly complicates the dynamics, consider first the case $E \lesssim 500$ MeV/nuc, where inelastic cross sections are small. In this case, relativistic kinematics can be neglected. Hence, meson degrees of freedom need not be treated explicitly, and the appropriate framework reduces to (non-relativistic) Quantum Many Body Theory with effective nucleon-nucleon potentials. However, except for the ground state and low lying excited states, this theory is also too difficult to apply.

To simplify further, note that quantum interference and off-shell effects are expected to be small if the deBroglie wavelength, $\lambda_E = 2\pi\hbar/\sqrt{2mE}$, is small compared to the typical mean free path, $\lambda = 1/(\sigma_{NN}\rho)$, between successive nucleon-nucleon collisions. For $E \sim (200 - 500)$ MeV/nuc, $\lambda \approx 2$ fm while $\lambda_E \approx (1 - 2)$ fm. Certainly

$\lambda_E << \lambda$ is not satisfied and classical dynamics cannot be justified on this basis. If nuclei were crystalline, then strong interference effects would be expected. However, it can be argued that nuclei are more like liquids, so that after many collisions phase information is lost. Thus to neglect interference effects a qualitative random phase argument must be invoked. To estimate the importance of off-shell effects, note that the finite time, $\lambda/v \sim (3\text{-}4)$ fm/c, between successive collisions leads to energy uncertainties $\Delta E = \hbar v/\lambda \sim (50 - 100)$ MeV. Thus $\Delta E/E \sim 25\%$, and the condition $\Delta E/E << 1$ is also only marginally satisfied. While the above considerations cannot then rigorously justify the applicability of classical dynamics, they can at least make its application somewhat plausible for $E \lesssim 500$ MeV/nuc. Actually, it would seem that the conditions justifying classical dynamics would be better satisfied for E > 500 MeV/nuc. However, the potential concept then loses significance and particle production cannot be neglected.

II.2 Classical Methods

Restricting then to $E \lesssim 500$ MeV/nuc, the general framework for classical dynamics is the Equation-of-Motion (EOM) method[7,9] with effective two body forces. While EOM has been demonstrated to be computationally feasible for heavy ion collisions and has the advantage of including collective effects, binding, correlations, and surface effects, such calculations are still in their preliminary stages. In particular, no result of EOM can be directly compared to data as yet. Therefore, still further idealizations are necessary.

Various approximations to EOM are possible depending on the time and length scales in the problem. See, in particular, Fig. I of Ref.(7).

For heavy ion collisions (E ~ 200 - 500 MeV/nuc) the following time scales are relevant:

1) τ_{int} = duration of individual NN collision

= force range r/c

$\approx 0(\hbar/m_\pi c) \sim$ (1-2) fm/c

2) τ_{rel} = relaxation time between successive NN collisions

$= \frac{\lambda}{v} \sim \frac{2fm}{(1/2-3/4)c} \sim$ (3-4) fm/c

3) τ_{col} = total collision time

$= \frac{L}{v} \sim \frac{10\ fm}{(1/2-3/4)c} \sim$ (10 - 20) fm/c

Note that the pion mass sets the scale for τ_{int} because OPE is the longest range nucleon force. For τ_{col}, L ~ 10 fm is the typical nuclear dimension traversed in central collisions.

While there are no gross differences between these time scales, the following inequality does seem to hold:

$$\tau_{int} < \tau_{rel} < \tau_{col} \qquad (1)$$

Rigorous approximations to EOM would follow[7] if any of the < signs in eq. (1) were replaced by <<.

Consider the three possible cases : A. $\tau_{int} \ll \tau_{rel}$, B. $\tau_{rel} \ll \tau_{col}$, and C. $\tau_{int} \ll \tau_{rel} \ll \tau_{col}$.

II.2(A) $\tau_{int} << \tau_{rel}$

In case A, only isolated two body collisions occur and collective effects are unimportant. This is the dilute gas limit. In this case EOM reduces to the Boltzmann equation or to intranuclear cascade, specified by free space NN cross sections. In heavy ion collisions, the condition $\tau_{int} << \tau_{rel}$ is rather marginally satisfied, especially when we consider the possible density dependence of the force range, r. In free space $r \sim \hbar/m_\pi c$, but in nuclear matter collective effects (polarization) can enhance r by a factor ~ 2 for $\rho \gtrsim 2\rho_o$. (See Ref. (10)).

II.2(B) $\tau_{rel} << \tau_{col}$

In case B, sufficiently many two body scatterings occur during the collision time that local thermal equilibrium can be assumed during the collision. In that case, EOM reduces[7,8] to hydrodynamics where nuclear interactions, binding and collective effects are described through an equation of state, $W(\rho,T)$. The condition $\tau_{rel} << \tau_{col}$ is best (although again marginally) satisfied for central collisions. Thus, for example, $U^{238} - U^{238}$ central collisions at 250 MeV/nuc should be fairly well described by hydrodynamics.

II.2(C) $\tau_{int} << \tau_{rel} << \tau_{col}$

Finally, the greatest simplification of EOM occurs in case C. In that case, EOM reduces to hydrodynamics with an ideal gas equation of state. There are then no compression effects and the excitation energy is distributed into translational and thermal energy. Clearly, this

case has the greatest potential with regard to formulating simple analytic models for heavy ion collisions. Unfortunately, the necessary condition $\tau_{int} << \tau_{rel} << \tau_{col}$ is also not well satisfied in eq. (1).

II.3 The need for a variety of models

Therefore, we are faced with the following dilemma: among all the tractable approaches that are possible in cases A, B, and C, none can be rigorously justified for heavy ion collision. Note, however, that eq. (1) does not rule out at least the partial validity of any of those approaches. Thus, the gross features of the data may turn out to be qualitatively reproduced, but the magnitude of the errors inherent in the methods cannot be estimated ahead of time. Recall also that this whole discussion was restricted to the case $E \lesssim 500$ MeV/nuc, where particle production is negligible. For $E > 500$ MeV/nuc, the only computationally feasible approaches are still those in cases A, B, and C. But these approaches are even less justified in that case.

Since no rigorous theoretical framework could be found for high energy heavy ion collisions, the best way to proceed is to turn to model calculations that include as many "realistic" effects as possible. The philosophy must then be shifted from seeking perfect agreement with data to providing background calculations that reveal the importance of particular (calculable) aspects of the dynamics. By varying the parameters within the models and by comparing results of different models, the sensitivity of the predictions to specific details can be determined. In this way, the most essential elements of the dynamics may perhaps be isolated. Therefore, we turn

in the next section to the consideration of a variety of dynamical models collected together for the first time in a Zoo of Models. The next section provides a guided tour of that zoo.

III. THE ZOO OF MODELS

The zoo of dynamical models is divided into the following sections:

1) Fireball - Westfall, et al., Ref. (11)
2) Firestreak - Myers, Ref. (12)
3) Hydrodynamics - Amsden et al., Ref. (8,13)
4) Row on Row - Knoll, Hüfner, Ref. (14)
5) Hard Spheres - Halbert, et al., Ref. (13,15)
6) Cascade 1 - Ginocchio, Ref. (13)
7) Cascade 2 - Smith, Danos, Ref. (16)

For the above models, results are available that can be compared directly with data. There are also incompleted sections of the zoo with models currently being developed. These are

8) Boltzmann eq. - Malfliet, Karant, Ref. (17)
9) Cascade 3 - Fraenkel, Ref. (18)
10) Equation of Motion, EOM 1 - Bodmer, et al., Ref. (7)
11) EOM 2 - Wilets, et al., Ref. (9)

A few models[19] have been omitted from the zoo because of space limitations.

The models (1-7) discussed in detail below are those that have been applied directly to the heavy ion homework problem (HI-HOPE) assigned at the end of the 3rd LBL Heavy Ion Summer Study, July 1976. The problem was to compute the proton inclusive cross section $d^2\sigma_p/d\Omega dE$ for the

reaction Ne + U → p + X at 250 and 400 MeV/nuc. These energies were chosen to optimize the chances of success of the possible approaches discussed in section II.2 (A-C). The proton inclusive $d\sigma_p$ was chosen because the composite, A = (d,α,etc.), inclusive cross sections, $d\sigma_A$ could be related to $d\sigma_p$ through $d\sigma_A \propto (d\sigma_p)^A$ in the coalescence model of Johansen, et al.[20] (An alternate model has since been developed by Mekjian[21] to explain this relation). Finally, these particular reactions were chosen so that direct comparison to data[11] would be possible.

Table I summarizes the essential features of models (1-7) and should be referred to during the following discussion for orientation. We begin the tour now in section 1.

III.1 Fireball[11]

This model is by far the simplest one and, therefore, involves the strongest assumptions. It falls in the category of section II.2(C). The main ingredients are (1) sharp sphere geometry, (2) relativistic kinematics, and (3) thermodynamics. For each impact parameter b, the projectile and target are assumed to make straight line, cylindrical cuts through each other (see Fig. Ia). The number of interacting nucleons, $N(b) = N_p(b) + N_T(b)$, from the projectile and target are thus determined by geometry. Relativistic kinematics then determine the center of mass momentum per nucleon, $p_{cm}(b)$, and the excitation energy per nucleon, $E^*(b)$, in terms of the beam energy, E. Finally, it is assumed that by the time, τ_{dis}, that the system disintegrates, sufficiently many two body scatterings will have taken place to thermalize the nucleon momentum distribution. Thus, at least by τ_{dis} the system has evolved into a "fireball".

Furthermore, a single temperature T(b) is assumed to specify the nucleon momentum distribution:

$$f(\tilde{p},b) = (2\pi mT(b))^{-3/2} \exp[-(\tilde{p} - \tilde{p}_{cm}(b))^2/(2mT(b))] \qquad (2)$$

Temperature and velocity gradients are neglected. An ideal gas equation of state is then used for $T(b) = 3(E^*(b) - B)/2$, where B = 8 MeV mocks up binding effects. The proton inclusive cross section is then given by

$$\frac{d^3\sigma}{dp^3} = \int_0^{R_P+R_T} 2\pi bdb\, N(b)\, f(p,b) \qquad (3)$$

To extend this model to energies E > 500 MeV/nuc, pions can be included by assuming[22] chemical as well as thermal equilibrium among pions and nucleons in the fireball. Then the mean pion multiplicity is given by

$$\langle n_\pi(b)\rangle = \int \frac{3V(b)d^3k}{(2\pi)^3}\left[e^{+\sqrt{k^2+m_\pi^2}/T(b)} - 1\right]^{-1} . \qquad (4)$$

The volume $V(b) = N(b)/\rho_c$ is the fireball volume at τ_{dis}, when the nucleon density has decreased to a "freeze out" density, $\rho_c \sim (1/4 - 1/2)\rho_o$. For $t > \tau_{dis}$ ($\rho < \rho_c$), no further interactions are assumed to take place, and the properties of the fireball are thus frozen out. The pion inclusive cross sections is then given by an expression similar to eq. (3). Note that T(b) must now be determined self consistently from $E^*(b) - B = 3/2T(b) + E_\pi(b)$, where $E_\pi(b)N(b)$ is the total energy stored in pions.

The fireball model can be extended even further to include composite (d,t,α,etc.) production,[21] without resorting to the coalescence model.[20] Assuming chemical equilibrium among all species, the relative abundances of various composites, for a fixed T(b), V(b), follow[21] from

the law of mass action. Here self-consistency is again essential to insure conservation of energy and baryon number.

III.2. Firestreak[12]

An extension of the fireball model to take temperature and velocity gradients into account is made in this model. The interaction region is divided into a series of tubes parallel to the beam axis. Each projectile tube is assumed to interact only with that target tube directly in its path (see Fig. Ib). Each tube-tube collision is then treated as in the fireball model. For each tube i, the number of nucleons $N(b,i) = N_P(b,i) + N_T(b,i)$ from the projectile and target is calculated. In this model, however, nuclear diffuseness can be easily included, and $P_{cm}(b,i)$ and $E^*(b,i)$ follow from kinematics. The key assumption is that in each tube-tube collision equilibrium is reached separately. This leads to a "firestreak" with gradients of velocity and temperature T(b,i) perpendicular to the beam. The proton inclusive cross section is then obtained by replacing $N(b)\ f(\tilde{p},b)$ in Eq.(3) by $\sum_i N(b,i)\ f(\tilde{p},b,i)$.

Pions and composites can also be included as in the fireball model with the further assumption that chemical equilibrium is eventually reached in each tube-tube collision separately. Such an extension of the firestreak model is currently being developed.[23]

Clearly, many "realistic" features of the dynamics are still missing from this model. In particular, no compression effects are included that lead, for example, to velocity and temperature gradients parallel to the beam. Furthermore, the neglect of interactions (viscosity) between adjacent tubes is questionable because of the high perpendicular momentum

transfers, $\langle \Delta P_\perp \rangle \sim 300$ MeV/c involved in typical NN collisions. The greatest virtue of this model remains in its obvious simplicity.

III.3 Hydrodynamics[8]

Turning now to the aquarium section of our zoo, we find a model that includes compression effects in a natural way. This approach is particularly appealing because (1) the conditions necessary for its application are at least approximately satisfied (sec. II.2 (B)), (2) it deals directly with $W(\rho,T)$, the object of our dreams (sec. I.1), and (3) effects of finite 3D geometry are included (though without surface diffuseness). Because of (2) and (3) the importance of at least two of the obstacles discussed in sec. I.2 - namely, loss of memory of $W(\rho,T)$ in asymptotic states and refraction effects - can in principle be determined. However, since the central assumption in (1-fluid) hydrodynamics is instantaneous (local) thermal equilibration, the importance of non-equilibrium dynamics cannot be determined.

III.3(A) 1-Fluid Model

The dynamical evolution of the system is assumed to follow from the continuity equations for the nucleon number $\rho(\vec{x},t)$, momentum $\vec{m}(\vec{x},t)$, and energy $e(\vec{x},t)$ densities:

$$\frac{\partial}{\partial t}\begin{pmatrix} \rho \\ \vec{m} \\ e \end{pmatrix} + \vec{\nabla}\cdot\begin{pmatrix} \vec{v} & \rho \\ \vec{v} & \vec{m} \\ \vec{v} & e \end{pmatrix} = \begin{pmatrix} 0 \\ -\vec{\nabla}P \\ -\vec{\nabla}\cdot(\vec{v}P) \end{pmatrix} , \qquad (5)$$

where $\vec{v}(\vec{x},t)$ is the velocity field and $P = \rho^2 \partial W(\rho,T)/\partial\rho$ is the pressure.

Equation (5) describes the simplest form of hydrodynamics with nonviscous flow and no dissipative effects. Such effects are negligible only if typical gradients are small compared to mean free paths, i.e. $|\vec{\nabla}f| << |f|/\lambda$ with $f = \rho,\vec{v},T$. The validity of this condition for heavy ion collisions is rather questionable,[7] especially if shock waves are generated. Corrections to Eq. (5) to order $\lambda|\vec{\nabla}f|/|f|$ lead to the Navier-Stokes equation. However, the solution of Eq. (5) already requires rather involved and costly numerical techniques.[8] Therefore, dissipative effects are neglected mostly on practical grounds.

For a specific model of $W(\rho,T)$, the following form was taken in Ref. (8):

$$W(\rho,T) = m_N + a(\rho/\rho_o)^{2/3} - b(\rho/\rho_o) + c(\rho/\rho_o)^{5/3} + I(\rho,T) \quad , \qquad (6)$$

with $(a,b,c) = (20,69,33)$ MeV corresponding to $W(\rho_o,0) - m_N = -16$ MeV and $K = 290$ MeV. For the internal (heat) energy, $I(\rho,T)$, the non-relativstic Fermi gas model was used. Note that Eq. (6) is a rather stiff equation of state with $W(\rho,0) - m_N \approx 100,200,300$ MeV for $\rho/\rho_o = 4,5,6$ respectively.

This model has been applied in detail for Ne + U at 250 MeV/nuc and also 2.1 GeV/nuc. The general features of the dynamics at 250 MeV/nuc (where hydrodynamics is most reliable) are particularly interesting. In Fig. II (taken from Fig. 2 of Ref. (8)), the time evolution of the collision is followed for central as well as peripheral collisions. Note first the $b = 0.1\ (R_{Ne} + R_U)$ case. By time 5.1×10^{-23}sec, a well defined Mach cone and shock region have formed. However, after refraction through the curved surfaces, little trace of the Mach cone remains. In fact, the final angular distribution (Fig. 4 of Ref. (8)) shows no peaks.

This proves the importance of refraction effects: the most interesting compression effects were washed out by them!

Figure II also shows that the idealizations of the fireball and firestreak models (Fig. I) are indeed crude. In particular the clean cut geometry is destroyed by the rapid spreading of the interaction region perpendicular to the beam.

Finally, the b ≃ 0.9 case illustrates a possible numerical instability in this model resulting in the striations in the target fluid. It serves as a warning that uncertainties in the results due purely to numerical technicalities are difficult to assess in this approach.

Up to now, $W(\rho,T)$ has not been varied in these calculations. Clearly, this should have top priority in future calculations.

III.3(B) 2-Fluids Model[24]

Moving on to the next tank, we encounter a hybrid model that is still basically macroscopic but has some microscopic aspects. The model simulates partial transparency during the collision by treating the projectile and target as distinct fluids. The fluids interact by exchanging energy and momentum at a rate that is estimated microscopically.

Consider a projectile element with density and velocity $(\rho_P,\vec{v}_P)$ colliding with a target element with $(\rho_T,\vec{v}_T)$. The average rate of NN collisions per unit volume in that element is $\rho_P\rho_T\sigma_{NN}\left|\vec{v}_P - \vec{v}_T\right|$ with $\sigma_{NN} \approx 40$ mb. In each collision a certain fraction[24] $\alpha \approx (1/4 - 1/2)$ of the relative momentum $m(\vec{v}_P - \vec{v}_T)$ is transferred from the projectile nucleon to the target one. Therefore,[24] the average momentum transfer rate per unit volume from

the projectile to the target fluids is given (non-relativistically) by

$$\langle \dot{\vec{m}}_{P\to T} \rangle \approx (\rho_P \rho_T \sigma_{NN} |\vec{v}_P - \vec{v}_T|)(\alpha m(\vec{v}_P - \vec{v}_T)) \quad . \tag{7}$$

A similar estimate gives the average energy transfer rate $\langle \dot{e}_{P\to T} \rangle$ with $m(\vec{v}_P - \vec{v}_T)$ replaced by $\frac{1}{2} m(v_P^2 - v_T^2)$ in Eq. (7).

The equations for the target fluid is then given by

$$\frac{\partial}{\partial t}\begin{pmatrix} \rho_T \\ \vec{m}_T \\ e_T \end{pmatrix} + \vec{\nabla} \begin{pmatrix} \vec{v}_T \rho_T \\ \vec{v}_T \vec{m}_T \\ \vec{v}_T e_T \end{pmatrix} = \begin{pmatrix} 0 \\ -\vec{\nabla} P_T + \langle \dot{\vec{m}}_{P\to T} \rangle \\ -\vec{\nabla} \cdot (\vec{v}_T P_T) + \langle \dot{e}_{P\to T} \rangle \end{pmatrix} \quad . \tag{8}$$

For the projectile, P and T interchange above.

The 2-fluids model is supplemented by a prescription when the relative velocity $|\vec{v}_P - \vec{v}_T|$ decreases below some critical velocity $v^* \approx c/3$. In that case the two fluids are assumed to mix into one, with further evolution governed by Eq. (5). It is hoped that the results are not sensitive to the details of this prescription.

Preliminary results are shown in Fig. III. Comparing with Fig. II, the effect of transparency is particularly noticeable at time 5.1. Note the absence of the Mach cone and the slower perpendicular spreading of the interaction region. Fewer particles seem to emerge in the backward directions; yet on the whole, by time 25.3, the one and two fluid results are remarkably similar. As discussed further in section III.8, $d^2\sigma_p/d\Omega dE$ also turns out to be rather similar in the two cases. This gives the first indication that the early, non-equilibrium phase of the collision has little effect on the asymptotic states. This will also be a recurring theme in other models.

III.4 Row on Row[14]

The next model we consider is also of hybrid variety. It has more microscopic details than the 2-fluids model, but at the same time neglects many "realistic" features such as compression effects and perpendicular spreading. Its main utility, for energies E < 1GeV/nuc, is in connection with the question of thermalization during heavy ion collisions and the sensitivity of results to microscopic details.

The projectile and target are subdivided into tubes or "rows" as in the firestreak model and again only straight line collisions between tubes are considered as in Fig. Ib. However, nucleons in each tube are now separately numbered as in Fig. IVa. The key assumption is that each projectile nucleon in a given row interacts once with every nucleon in the target row. Collisions between two projectile or two target nucleons are neglected, i.e., no pile-up of density. The idea is to follow the linear cascade of each projectile nucleon separately.

The momentum distribution of the m^{th} projectile nucleon after colliding with n target nucleons is denoted by $W^P_{mn}(\tilde{p}_P)$. Similarly, $W^T_{mn}(\tilde{p}_T)$ is the distribution of the n^{th} target nucleon after being scattered by m projectile nucleons. Given the transition probability $M(\tilde{p}_P\tilde{p}_T \to \tilde{p}_P'\tilde{p}_T')$ for NN scattering, $M \propto d\sigma_{NN}/d\Omega_{cm}$, W^P_{mn} is then related to $W^T_{m-1,n}$ and $W^P_{m,n-1}$ by

$$W^P_{mn}(\tilde{p}_P') = \int d^3p_T' \, d^3p_P \, d^3p_T \quad W^P_{m,n-1}(\tilde{p}_P) \, W^T_{m-1,n}(\tilde{p}_T) \times M(\tilde{p}_P,\tilde{p}_T \to \tilde{p}_P' \; \tilde{p}_T') \quad . \tag{9}$$

Because of the complexity of Eq. (9), it is solved by a moments expansion. However, only the moments $\langle p_{\|} \rangle^i_{mn}$, $\langle \sigma_{\|}^2 \rangle^i_{mn}$ and $\langle \sigma_{\perp}^2 \rangle^i_{mn}$ are calculated

explicitly from the recursion relations that follow[14] from Eq. (9). For example,

$$\langle p_{\parallel} \rangle^{P}_{mn} = (1 - S^2) \langle p_{\parallel} \rangle^{P}_{m,n-1} + S^2 \langle p_{\parallel} \rangle^{T}_{m-1,n} \quad , \tag{10}$$

where $S^2 = \langle \sin^2(\theta_{cm}/2) \rangle_{NN}$ is a particular moment of $d\sigma_{NN}/d\Omega_{cm}$ and is essentially the fractional longitudinal momentum loss per collision. Recursion relations for the $\langle \sigma^2 \rangle$ involve another moment, $\beta = \langle \frac{1}{4} \sin^2 \theta_{cm} \rangle$, as well, but they are too cumbersome to reproduce here.[14] Thus S^2 and β are the only inputs from experiment. For a given row on row as in Fig. IVa, the recursion relations are solved, and the form of the $W^{i}_{mn}(\tilde{p})$ are assumed at the end to be uniquely determined by those three moments:

$$W(\tilde{p}) = [(2\pi)^{3/2} \langle \sigma_{\parallel}^2 \rangle^{1/2} \langle \sigma_{\perp}^2 \rangle]^{-1} \exp\left\{ - \frac{(p_{\parallel} - \langle p_{\parallel} \rangle)^2}{2\langle \sigma_{\parallel}^2 \rangle} - \frac{p_{\perp}^2}{2\langle \sigma_{\perp}^2 \rangle} \right\} \tag{11}$$

The results of such a procedure are illustrated in Fig. IVb (from Fig. 10 of Ref. (14)) for a collision of a row of 3 nucleons and a row of 8 nucleons at 400 MeV/nuc. The numbered arrows indicate the $\langle p_{\parallel} \rangle$ for the different nucleons. Complete thermalization as in the firestreak model implies that all distributions are identical and given by the short dashed curve (normalized back to unity). While the linear cascade did not reach the thermal limit for each nucleon separately, note the remarkable similarity of the summed distribution to the firestreak result. This shows how insensitive the single particle inclusive cross section is to the degree of thermalization. In fact, if sufficiently many collisions

occur so that $\langle\sigma_{\parallel}^2\rangle \approx \frac{1}{2}\langle\sigma_{\perp}^2\rangle$, then energy and momentum conservation alone determine $\langle p_{\parallel}\rangle$ and $\langle\sigma_i^2\rangle$. The form of W, Eq. (11), then follows from the central limit theorem of statistics. Thus with energy, momentum conservation and a few collisions per nucleon, the summed distribution $(d^2\sigma_p/d\Omega dE)$ cannot deviate much (by factor $\lesssim$ 2) from the extreme thermal result.

In Ref. (14) the sensitivity of the results to S^2 and β, (i.e., the microscopic details of the collision) was also studied. It was shown (cf. Fig. 11, Ref. (14)) that, they are insensitive to those parameters as long as the stopping distance $\lambda_{stop} = \lambda/S^2$ is less than typical row lengths L. Thus, what is meant by "sufficiently many" collisions above is "more than $1/S^2$". The insensitivity of $d^2\sigma_p/d\Omega dE$ to microscopic details of the collision for $L/\lambda_{stop} \gtrsim 1$ is in accord with the 2-fluid results.

III.5 Hard Spheres or SIMON Says[15]

In this and subsequent sections of the zoo, the microscopic models are found. These are all classical cascade approaches (cf. sec. II.2(a)), that follow the development of two body collisions in the system. They all use Monte Carlo techniques and involve lengthy computer codes (whose numerical reliability ("bugs") is difficult to assess).

Hard spheres is one of three options for the NN scattering mechanism that is part of a code called SIMON.[15] All mechanisms considered in this model are idealized NN elastic cross sections. They are (1) hard spheres with diameter 0.9 fm $\Rightarrow \sigma = 25$ mb, (2) repulsive impact scattering, RIS, with a, $r_c = 0.25$ fm, hard core, (3) RIS without hard core.

In the RIS mechanism, scattering occurs at the instant that the separation between two nucleons decreases to their impact parameter b , as long as $b \leq 0.9$ fm. For $b > 0.9$ fm no scattering takes place. In case (2), hard sphere scattering occurs if $b \leq 2r_c$. Otherwise, the nucleons are scattered randomly over 4π solid angle at that point. While mechanisms (2) and (3) are slightly more realistic, the hard sphere one is of particular interest because the equation of state of a hard sphere gas is very different from ones such as in Eq. (6). For example for $T = 0$ and $\rho/\rho_o = 10$, $W(\rho/\rho_o \lesssim 15, 0) - m_N = 0$ for hard spheres whereas in Eq. (6) $W(10,0) - m_N \approx m_N$! Therefore comparing hard sphere results to hydrodynamics will give much insight into the sensitivity of the results to the equation of state.

A feature of this method that differentiates it from other cascade models is that two nucleons certainly scatter if $b < 0.9$ fm. In the other cascades there is only a finite probability, $1/\lambda = \sigma_{\ldots}$ of scattering per unit length. As a result many more two body collisions occur in this approach than in the other cascades. For example, in the hard sphere model so many violent collisions take place that densities ρ were found[15] to be limited to $\lesssim 2\ \rho_o$ in calculations of U-U central collisions. This should be contrasted to maximum compressions $\rho \gtrsim 4\ \rho_o$ attained in hydrodynamics. Note the apparent paradox that ρ_{max} (hard sphere) $< \rho_{max}$ (hydro) while $W_{\text{hard sph.}}(\rho,0) < W_{\text{hydro}}(\rho,0)$ for $2\rho_o \lesssim \rho \lesssim \rho_s \approx 15\ \rho_o$. In fact for the three mechanisms above, $W = 3/2\ T$ (ideal gas) for $\rho < \rho_s$. Yet ρ_{max} ($\approx 2,3,3.5$) also differs[15] for the three mechanisms. This paradox is resolved[25] when one notes that the dynamical driving term in Eqs. (5,8) is the pressure $P = \rho^2\ \partial W/\partial\rho$ evaluated at

constant entropy, S. Therefore, even though $\partial W/\partial\rho|_T = 0$ for $\rho < \rho_s$, $P = \int^{\rho}\partial W/\partial\rho|_S = \rho T(1 - \rho/\rho_s)^{-1}$ in the dilute limit for hard spheres. This illustrates that the dynamics at a given density, ρ, is not fully determined by $W(\rho,T)$ at that ρ.

II.6 Cascade 1[13,26]

In this model, detailed experimental cross sections are used as input for the first time. In particular, pion production and absorption are treated explicitly through isobar production. Binding effects are also included.

The central assumption is that nucleus-nucleus ($A_P + A_T$) collisions can be approximated by the superposition of A_P independent nucleon-nucleus ($p + A_T$) collisions. Collisions between cascading particles are therefore neglected. Hence, the pile-up of density is ignored..

Each $p + A_T$ collision is processed by the VEGAS code[27] that reproduces $p + A_T$ data over a wide range of energies and targets. An important feature of this code is the optical potential that acts to absorb cascade nucleons. Thus, for example, in p + U at 250 MeV the average number of target nucleons that scatter is found[26] to be ≈ 6.7. On the other hand, the number of cascade nucleons that finally leave the nucleus is ≈ 2.2. Hence, $\approx 70\%$ of the cascading nucleons are reabsorbed by the optical potential.

In heavy ion collisions, though, both projectile and target disintegrate after colliding (see, Fig. II,III). Therefore, no optical potential survives to absorb nucleons. Since the normalization of the proton inclusive cross section is proportional to the nucleon multiplicity, we can expect Cascade 1 to underestimate the proton inclusive by at least a factor ~ 3. Furthermore, compression effects lead to smaller mean

free paths, $(\sigma\rho)^{-1}$, and, hence, even more collisions. The absence of this effect also leads to an underestimate of $d^2\sigma_p/dEd\Omega$. Indeed, results[13] with Cascade 1 are found to be ~ 5 times smaller than data for Ne + U at 250 MeV.

We note that improvements on this method are currently being developed in Ref. (18).

III.7 Cascade 2[16]

This is by far the most ambitious and microscopic model in the zoo. The simultaneous evolution of all projectile and target cascade particles is followed. Pion production and absorption are included via $NN \rightleftarrows N\Delta$, and experimental cross sections are used to determine the outcome of two body collisions. Diffuse nuclear surface, Fermi motion, the exclusion principle, and binding effects are also included.

However, the price paid for all these features is high. They necessitate a very complex and expensive computer code, whose detailed workings are beyond the grasp of nontechnicians. It is therefore difficult to judge which results are real physical effects and which are consequences of specific numerical procedures. The methods used in Cascade 2 are novel and differ from conventional[27] cascade approaches. Consequently, they are also subject to the dictum: "Guilty - until proven innocent".

Tests of Cascade 2 on p + A data in fact indicate that the method is not free of difficulties yet. Very preliminary results[28] for p+Pb → p+X at 740 MeV show that Cascade 2 is consistently higher than Cascade 1 (which agrees with data) by a factor ~ 2. Furthermore, very preliminary

results of Cascade 3, Ref. (18), indicate that Cascade 2 is also consistently higher than Cascade 3 for Ne + U at 250 MeV/nuc - although in that case, Cascade 2 agrees with the data (see sec. III.8). Thus, Cascade 2 has not been proven innocent yet.

However, many results are available that are very instructive regardless of the above reservations. Figure V (Fig. (3) of Ref. (16)) shows the time evolution of various quantities for Ne + U. N_P and N_T are the number of projectile and target nucleons that have scattered at least once. N_B and N_F are the number of bound and free cascading nucleons. The total number of cascading nucleons $N = N_P + N_T = N_B + N_F$ is also shown. Arrows indicate the average number of collisions per nucleon.

Note case b = 0 in particular. After a time ~ 15 fm/c, $N_P \approx 20$ and all projectile nucleons have interacted at least once. N_T continues to increase rapidly ($dN_T/dt > A_P c/\lambda \approx 10$ c/fm) indicating that recoil target nucleons scatter with other target nucleons as well. By ~ 30 fm/c, an average of 3 collisions per nucleon have taken place and N_T begins to level off as cascading nucleons start leaking out of the target. By ~ 40 fm/c, the collision is essentially over. Note however that only $N \approx 100$ nucleons have participated in this central collision. What happened to the ≈ 158 other nucleons in the system? They remain in a target full of holes where NN collisions have taken place. This "Swiss cheese" remnant is an unwanted by-product of Cascade 2. It is assumed that nucleons emerging from that remnant contribute only to the unobserved, low energy (E < 20 MeV) part of the spectrum.

Turning to the predicted proton spectrum, Fig. VI (Fig. (5) of Ref. (16)), the degree of thermalization can be analyzed. The results are presented in terms of Lorentz invariant cross sections with

$v_\perp = p_\perp/m$ and $y = \tanh^{-1}(v_\parallel/c)$. The solid curves give the best fit assuming an isotropic thermal distribution in a frame moving with velocity βc. Complete thermalization would imply that the perpendicular and parallel temperatures ($\tau_\perp$ and $\tau_\parallel$) are equal. For b = 0, this is nearly the case, but for b = 9 fm, $\tau_\parallel \approx 1.6\ \tau_\perp$ and thermalization is not achieved. The bdb averaged distributions also show incomplete thermalization.

A final point that should be stressed in connection with Cascade 2 is its great utility as a tool for study of the dependence of results on specific microscopic details. Thus, for example, the effects of enhanced NN cross sections due to possible pionic instabilities[10] can be studied with this method.

III.8 Comparison of Results

The results of the various models in sections III.1-7 will now be compared for the reaction Ne + U → p + X.

In order to compare the data[11], the proton inclusive data should be first corrected for coalesced[20] nucleons. This is because composite (d,α,...) fragment production was not taken into account thus far in any of the model calculations for this reaction. Consequently, the predicted proton spectrum should be compared to the "primeval" spectrum, before any nuleons have coalesced[20]:

$$d\sigma_{primeval} = \sum_{Z,N} Z\, d\sigma_{exp}(Z,N) \qquad (12)$$

where $d\sigma_{exp}(2,1)$ is, for example, the measured[20] single particle ^{3}He inclusive cross section. This "coalescence" correction turns out to be important ($d\sigma_{primeval}/d\sigma_{exp}(1,0) \approx 2$-3) for low energy protons, $E_{lab} \lesssim 50$ MeV.

In Fig. VII (Fig. (6) of Ref. (12)) the results of the Fireball (dashed) and Firestreak (solid) models are compared. The T and $\vec{v}$ gradients of the Firestreak model seem to have very little effect in the results. However, this is most likely due to the impact parameter summation in Eq. (3). T(b) varies with b for Ne + U at 250 MeV/nuc over a range 24 ~ 33 MeV in the Fireball model[11]. This large variation of T(b) obscures the effect of spatial variations of T for each b. The greatest differences between these models should therefore arise for equal mass systems. In that case, T(b) and $p_{cm}(b)$ are constants in the Fireball model. Indeed, preliminary results[29], Fig. VIII, for U-U collision at 250 MeV/nuc show much larger (factor 2-5) differences between the two models. This point illustrates how impact parameter averaging can in certain cases (Ne + U) wash out many differences between the models.

Next we compare results of 1-fluid hydrodynamics and hard spheres in Fig. IX (Fig. (1) of Ref. (13)). Note the great similarity between the results of these two models even though their equations of state, $W(\rho,T)$, are so different! This was one of the fears expressed in sec. I.2. At least, the b averaged proton inclusive seems completely insensitive to $W(\rho,T)$.

Furthermore, the results[24] of the 2-fluids model (see Fig. X) do not differ very much from the 1-fluid results. Thus, $d\sigma_p$ does not seem to be sensitive to non-equilibrium stages of the collision. This insensitivity of the results to pre-equilibrium dynamics was also found in Row on Row model, Fig. 7 of Ref. (14) and Fig. IVb. The proton inclusive spectrum in this model is therefore also very similar to results of the Fireball and streak models.

The results of Cascade 1 and 2 are also shown in Fig. IX. As expected from sec. III.6, Cascade 1 is consistently too low, indicating that $A_p + A_T$ collisions are not simply A_p independent $p + A_T$ collisions. (This is actually a positive result - we do not have to close up shop on heavy ion collisions yet!) Cascade 2, on the other hand, is too high in general. However, subsequent modifications of Cascade 2 and improved statistics have resulted in excellent agreement with data - as shown in Fig. XI (Fig. (1) of Ref. (16)). The agreement is further improved when the data are coalescence corrected. An open question is whether that agreement will remain after existing bugs (see sect. III.7) in Cascade 2 are eliminated.

On the whole though, the proton inclusive data seems to be invariant to the details of the models to within a factor ~ (2-3). One reason for this model independence is the impact parameter summation as noted in connection with the Firestreak model. This is also clear from Fig. XII (Fig. (3) of Ref. (13)), which specifically shows results for b = 0. Note how much more the results of the 1-fluid and hard spheres models differ here than in b averaged case Fig. IX. It is therefore very desirable to get data in the future which are mostly biased to central collisions.

IV. SUMMARY AND OUTLOOK

The purpose of this report has been to provide a general introduction to the models of high energy heavy ion collisions. Clearly many topics and models have been omitted. We have focused here on those models that have been applied to the heavy ion homework problem (Ne + U → p + X at 250 and 400 MeV/nuc). These ranged from the extremely simple Fireball to the very complex Cascade 2.

First we found in sect. II that none of the methods could be rigorously justified. However, Eq. (1) gave some hope that they were at least partially valid for energies 100 - 500 MeV/nuc. The comparison to data in fact showed that most models could reproduce the gross features of the data to within a factor of 2-3. To a large extent though, the impact parameter summation helped to hide many detailed differences between the models. Also, because every projectile nucleon could be effectively stopped in the target, the results of many models approached the thermal limit.

We also considered the question of whether $W(\rho,T)$ could be deduced from heavy ion collisions. In sec. III.5, we encountered several models with the same $W(\rho,T)$ over a finite range ($\rho < \rho_s$) of densities that led to different results. The different dynamics were due,[25] in those cases, to different entropy $S(\rho,T)$ functions leading to different pressures $\rho^2 \partial W/\partial \rho|_S$. Knowledge of W alone over a finite region of densities is therefore not sufficient to determine the dynamics. In that case, the pressure or S must also be known independently. This of course makes simple extraction of W from heavy ion collisions very difficult.

Even if W cannot be determined accurately, qualitative differences between the models can be accentuated by concentrating on b = 0. There is clearly no point in considering impact parameter summed quantities in the future. Experimentally, equal mass, A + A, projectile-target combinations optimize the chances for devising a $b \approx 0$ trigger. In particular, one expects that azimuthal symmetry, coupled with very high ($\sim 2A$) multiplicities, can result only from head on collisions. Theoretically, b = 0 collisions of A + A systems are also expected to magnify the qualitative differences between the models. A simple qualitative

measure of those differences is given by the theta asymmetry, $\eta = [Y(0^\circ) - Y(90^\circ)]/[Y(0^\circ) + Y(90^\circ)]$, where $Y(\theta_{cm}) = d\sigma_p/d\Omega_{cm}$. (One practical advantage of A + A system is that the center of mass, CM, corresponds to the nucleon-nucleon CM.) For the row on row and cascade models $\eta > 0$; for the fireball and firestreak, $\eta = 0$; for 1-fluid, hard spheres, and EOM[7] $\eta < 0$. It is hard to guess η for 2-fluids. The great similarity of the firestreak and 2-fluids models in Fig. VII is most likely due to the b summation. It would be very desirable to compare the $b = 0$ contributions in the CM system!

In this report, we have not discussed the energy range 0.5 - 2 GeV/nuc because (1) the models are even less justified there than at energies $\lesssim$ 500 MeV/nuc, and (2) most calculations and experiments are still in a very preliminary stage. The interesting new observables in this energy range are the pion inclusive cross sections and the pion multiplicity distributions. Preliminary results[22,31] for these b summed observables indicate that many diverse models can fit the data. This points again to the necessity of isolating head on, A +A collisions in order to differentiate between the models.

Finally, we comment on the likelihood of observing exotic phenomena as discussed in sec. (I.1). Unless spectacular long lived density isomeric states are produced in conjunction with enormous π multiplicities, it appears that clear cut evidence for unusual phenomena will be hard to extract from single particle observables. For example, pionic instabilities[10]

can lead to (2 ~ 4 times) enhancements of the effective NN cross sections in the medium. However, preliminary results[33] of Cascade 2, employing such enhanced cross sections, indicate that only ~ 50% effects on the b summed proton inclusive distribution and $\lesssim$ 20% effects on the pion multiplicities can be expected. There is hope, however, that multiparticle correlations[30] will be much more sensitive to unusual dynamical mechanisms. Thus, in addition to restricting to b = 0, A + A collisions, observables such as the two or three particle inclusive spectra should be considered in the future.

Acknowledgements:

Most of the analysis contained in this report arose out of numerous private discussions. I am particularly grateful to J. N. Ginocchio, A. S. Goldhaber, W. D. Myers, J. R. Nix, and R. K. Smith for making their unpublished results and views known to me. Valuable conversations with N. K. Glendenning, S. K. Kauffmann, and Y. Karant are also gratefully acknowledged.

This work was done with support from the U.S. Energy Research and Development Administration.

TABLE I: Overview of Models

I. Macroscopic: Assumes local thermal equilibrium

- A. Ideal gas $W(\rho,T)$ - no compression effects
  - (1) Fireball - no $T,\tilde{v}$ gradients
  - (2) Firestreak - with $T,\tilde{v}$ gradients
- B. Realistic $W(\rho,T)$ - finite K
  - (3a) 1 - fluid Hydrodynamics

II. Semi-Microscopic: Finite mean free path

- A. Continuum with partial equilibrium
  - (3b) 2 - fluid Hydrodynamics
- B. One dimensional analytic cascade
  - (4) Row on Row

III. Microscopic: Input NN cross sections, employ Monte Carlo methods

- A. Ideal classical cascade
  - (5) Hard Spheres
- B. With measured cross sections
  - (6) Cascade 1 - superposition of p+A cascade
  - (7) Cascade 2 - full intranuclear cascade

REFERENCES

1. See the review of high energy heavy ion experiments by H. Heckmann elsewhere in these proceedings. An experimental review is also being prepared by R. Stock currently.

2. Two separate reviews on theoretical developments are also currently being prepared by A. S. Goldhaber and J. R. Nix.

3. T. D. Lee and G. C. Wick, Phys. Rev. D9, 2291 (1974); Rev. Mod. Phys. 47, 267 (1975); A. K. Kerman, L. D. Miller, LBL-3675 report, p. 73, (1975), unpublished; E. M. Nyman, M. Rho, Nucl. Phys. A268, 408 (1976); J. Bogrita, "Remarks on Nuclear Density Isomers in Infinite Nuclear Matter," Argonne preprint (1977).

4. Zero temperature pion condensation:
A. B. Migdal, D. A. Markin, I. I. Mishustin, Sov. Phys. JETP 39, 212 (1974).
G. E. Brown, W. Weise, Phys. Reports 276, 1 (1976).
J. M. Irvine, Rep. Prog. Phys. 38, 1385 (1975);
Finite T condensation: V. Ruck, M. Gyulassy, W. Greiner, Z. Phys. A277, 391 (1976).

5. G. F. Chapline, M. Nauenberg, UCRL-79090 preprint, "On Possible Existence of Quark Stars."

6. H. G. Baumgart, J. U. Schott, Y. Sakamoto, E. Schopper, H. Stödser, J. Hofmann, W. Scheid, W. Greiner, Z. Phys. A273 359 (1975).

7. A. R. Bodmer, C. N. Panos, Phys. Rev. C15 1342 (1977); A. R. Bodmer, Proceedings of the Meeting on Heavy-Ion Collisions, Fall Creek Falls, Tennessee (June 1977).

8. A. A. Amsden, F. H. Harlow, J. R. Nix, "Relativistic Nuclear Fluid Dynamics", Los Alamos Lab Report LA-UR-77-31 (January 1977).

9. L. Wilets, E. M. Henley, M. Kraft, A. D. MacKellar, Nucl. Phys. A282, 341 (1977).

10. M. Gyulassy, W. Greiner, "Pions Instabilities and Critical Scattering Phenomena in Heavy Ion Collisions", University of Frankfurt, Germany, preprint (January 1977) to appear in Ann. Phys.; M. Gyulassy, LBL-6525 preprint, to appear in Proceedings of Meeting on Heavy Ion Collisions, Fall Creek Falls, TEnnessee (June 1977).

11. G. D. Westfall, J. Gosset, P. J. Johansen, A. M. Poskanzer, W. G. Meyer, H. H. Gutbrod, A. Sandoval, R. Stock, Phys. Rev. Lett., 37, 1202 (1976); J. Gosset, et al., LBL-5820 preprint (1977).

12. W. D. Myers, "A Model for High Energy Heavy Ion Collisions, LBL-6569 preprint (August 1977).

13. A. A. Amsden, J. N. Ginocchio, F. H. Harlow, J. R. Nix, M. Danos, E. C. Halbert, R. K. Smith, Phys. Rev. Lett. 38, 1055 (1977).

14. J. Hüfner, J. Knoll, "Rows on Rows - Theory of Collisions between Heavy Ions at High Energy," University of Heidelberg preprint (1977).

15. J. P. Bondorf, H. T. Feldmeier, S. Garpman, E. C. Habert, Phys. Lett. 65B, 217 (1976); Z. Phys. 279, 385 (1976);

16. R. K. Smith, M. Danos, Proceedings of Meeting on Heavy Ion Collisions, Fall Creek Falls, Tennessee (June 1977); and to be published.

17. R. Malfliet, Y. Karant, to be published.

18. Z. Fraenkel, to be published.

19. S. E. Koonin, Phys. Rev. Lett. 39, 680 (1977).

19. (cont.)

I. A. Schmidt, R. Blankenbeckler, Stanford University preprint SLAC-PUB-1881, "Relativistic Interactions Between Nuclear," (Feb. 1977); these modeis apply to the high energy fragment yields.

20. H. H. Gutbrod, A. Sandoval, P. J. Johnasen, A. M. Poskanzer, J. Gosset, W. G. Meyer, G. D. Westfall, R. Stock, Phys. Rev. Lett. 37, 667 (1976).

21. A. J. Mekjian, Phys. Rev. Lett. 38, 604 (1977); and "Explosive Nucleosynthesis, Equilibrium Thermodynamics and Relativistic Heavy Ion Collisions", LBL-6545 preprint (June 1977).

22. J. I. Kapusta, "Particle Production in the Nucleus Fireball Model," LBL-6504, preprint 1977; and to be published.

23. J. Kapusta, G. Westfall, J. Gosset (to be published).

24. A. A. Amsden, A. S. Goldhaber, F. H. Harlow, J. R. Nix (to be published).

25. I am grateful to A. Goldhaber for discussion on this point.

26. J. N. Ginocchio (to be published).

27. G. O. Harp, et al., Phys. Rev. C 8, 581 (1973); Phys. Rev. C 10 2387 (1974); H. W. Bertini et al., Phys. Rev. C14 590 (1976).

28. J. N. Ginocchio, R. K. Smith, private communication.

29. Unpublished Fireball + streak results were calculated W. D. Myers[12]; hydrodynamic results are due to Amsden, et al.[24]

30. S. E. Koonin, "Proton Pictures of High-Energy Nucleus Collisions," NBI-77-13 preprint (1977).

31. M. Gyulassy, S. K. Kauffmann, "Pion Multiplicity Distributions in Heavy Ion Collisions," LBL-6593 preprint, Sept. (1977).

32. An intriguing possible way of detecting density isomerism was considered by J. Hofmann, H. Stöcker, U. Heinz, W. Sheid, W. Greiner,

32. (cont.)

Phys. Rev. Lett. 36, 88 (1976). This is based on observing Mach cones.[6] However, refraction effects (sec. II. 3(A)) are likely to smear out angular distributions, and some experiments (Ref. (11) and H. Hekcmann, Proceeding of Fall Creek Falls Meeting on Heavy Ion Collision (June 1977)) have not been able to find evidence for Mach cones.[6] This remains a controversial topic today.

33. R. K. Smith, private communication.

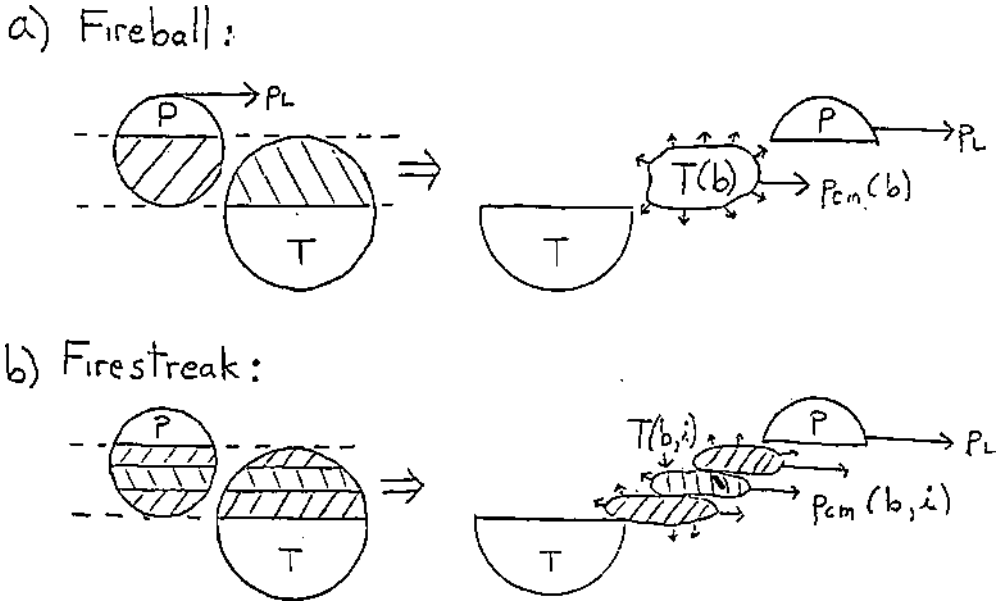

Fig. 1. Geometry of Fireball (a) and Firestreak (b) models.

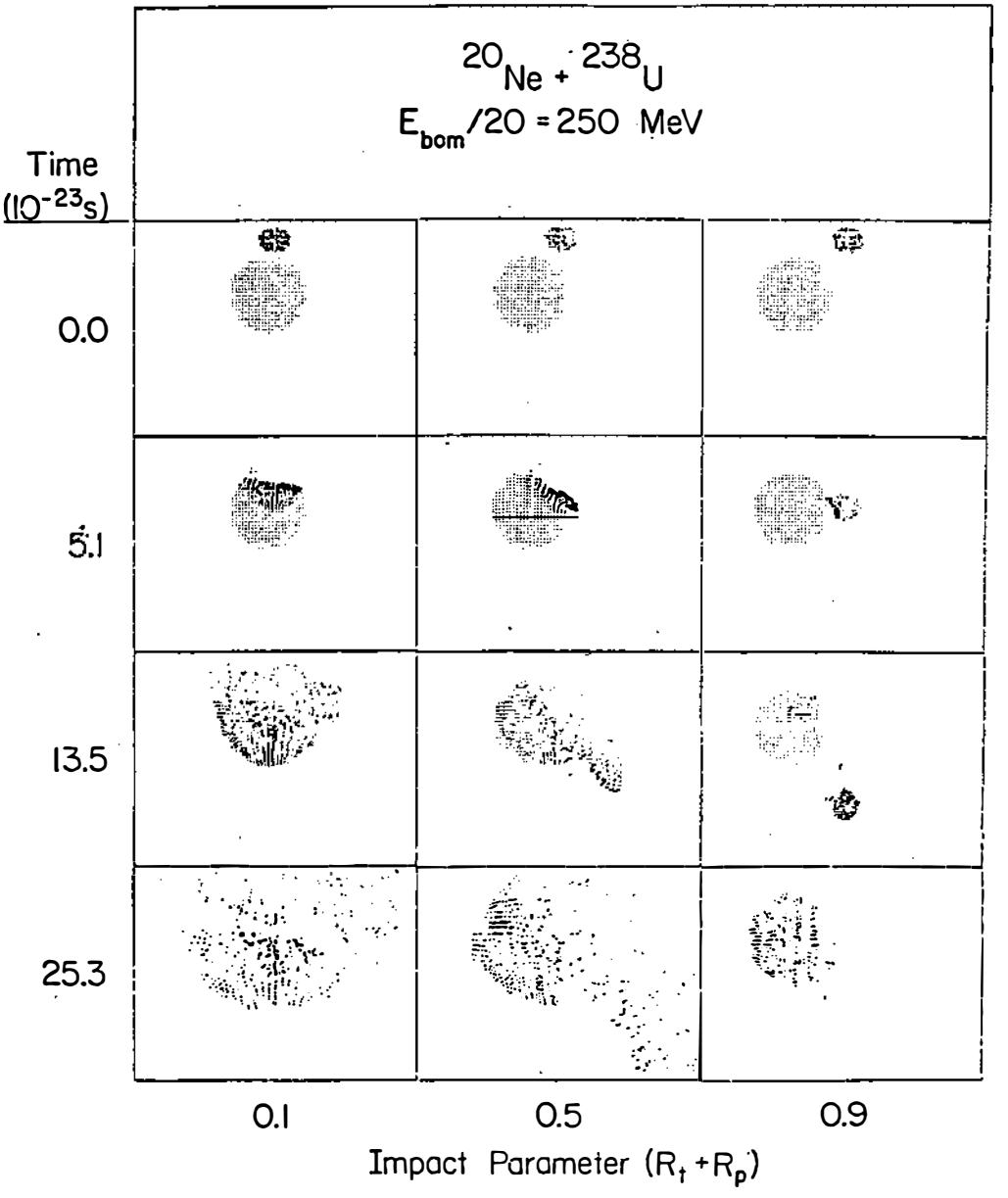

Fig. 2. Results of 1-fluid model for Ne + U (Fig. 2, Ref. (8)), darker shades correspond to higher densities.

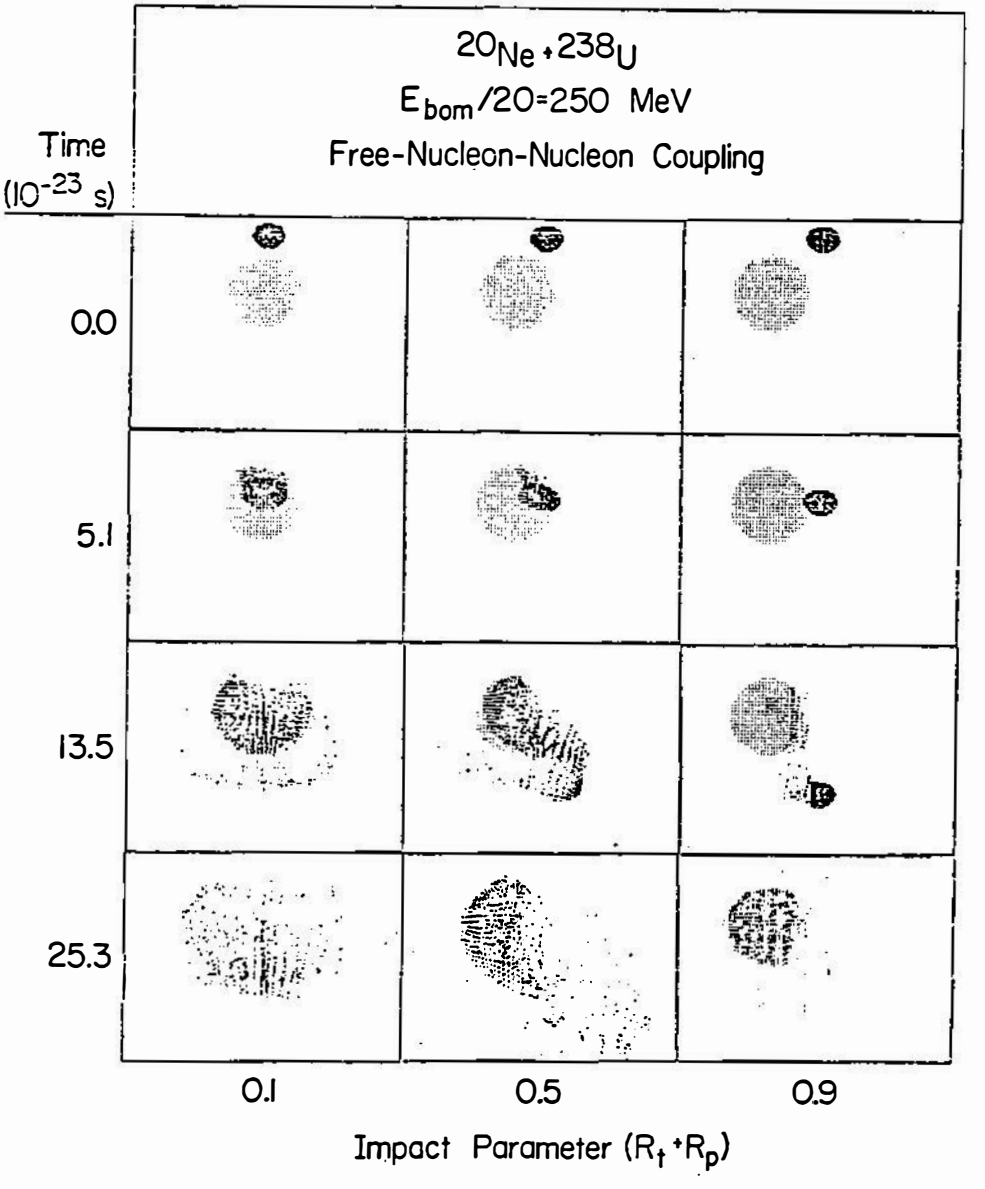

Fig. 3. Results of 2-fluids model[24] for same reaction as in Fig. 2.

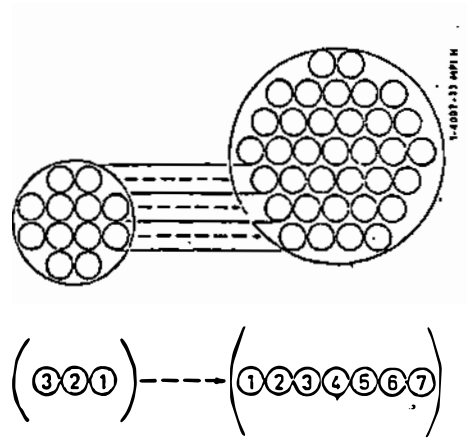

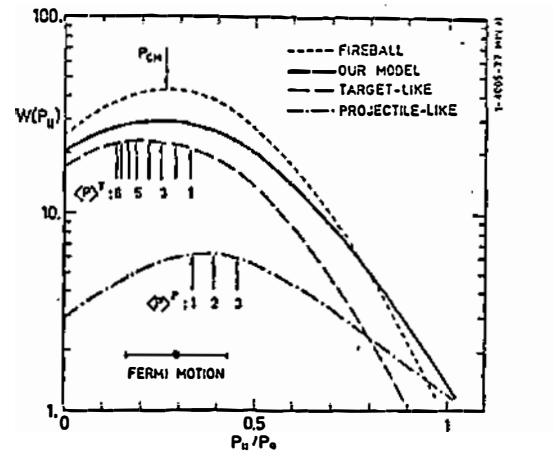

Fig. 4. (a) Geometry of Row on Row model (Fig. 2, Ref. (14)
(b) Distribution of longitudinal momenta for scattering of a row of 3 nucleons by a row of 8 at 400 MeV/nuc. Projectile and target distributions are shown separately (Fig. 10, Ref. (14)).

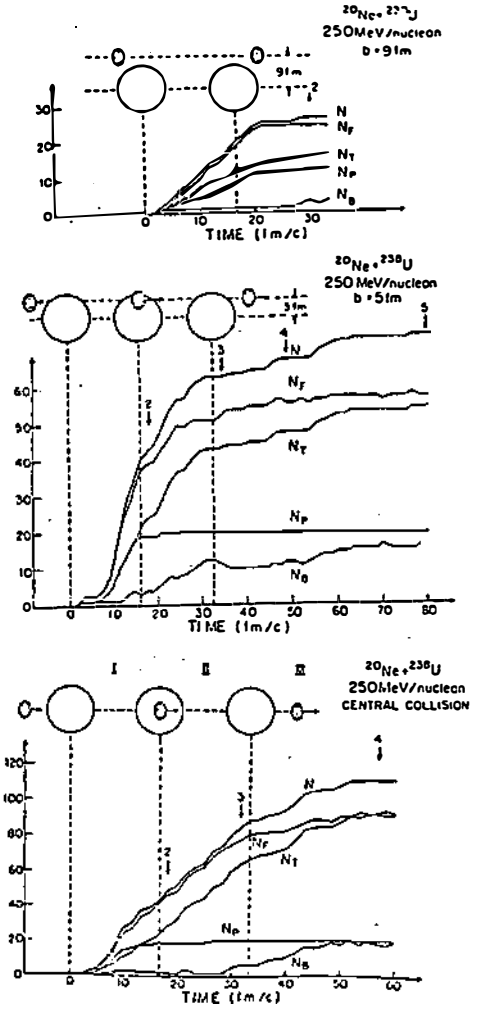

Fig. 5. Number of particles N that have interacted at least once in Cascade 2 for Ne + U at various impact parameters. N is decomposed into the number from the projectile N_p and target N_T. The number of bound N_B and free N_F particles are also indicated (Fig. 3, Ref. (16)).

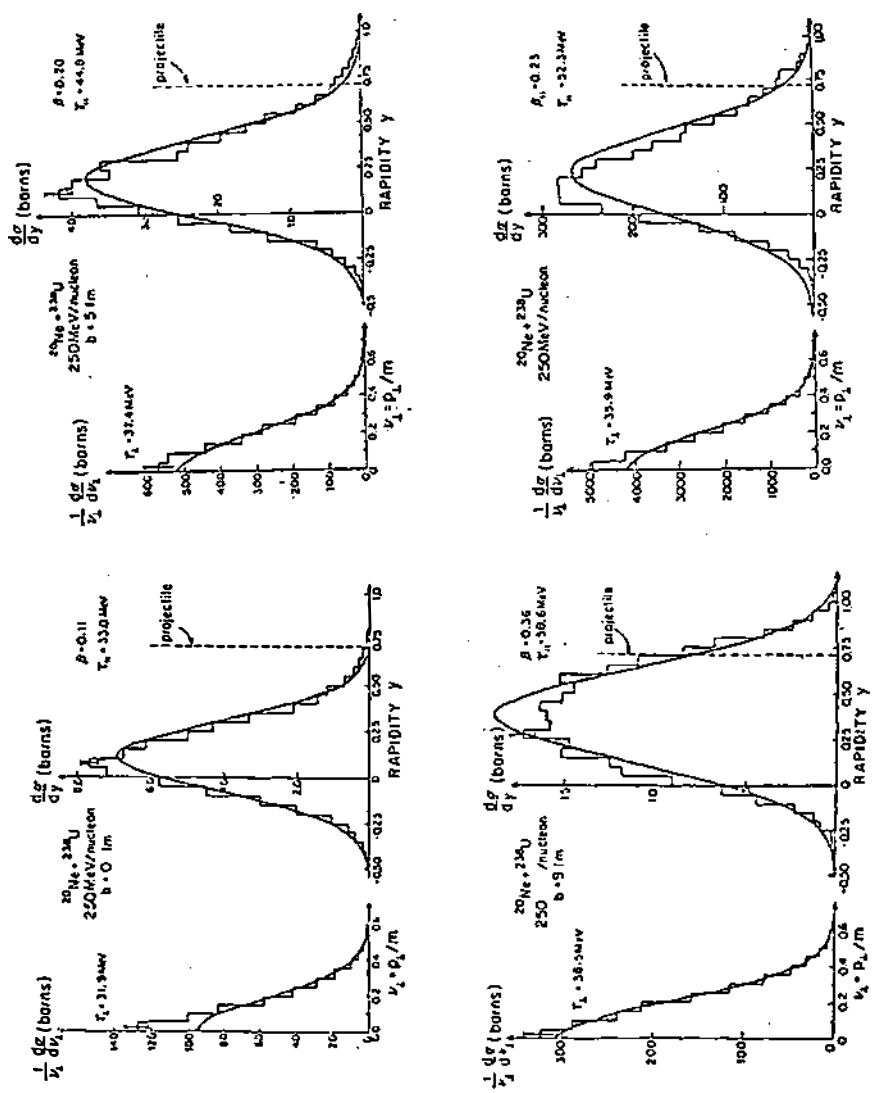

Fig. 6. Transverse and longitudinal distributions for different impact parameters and the total spectrum. The solid curves are fits with Boltzmann distributions.

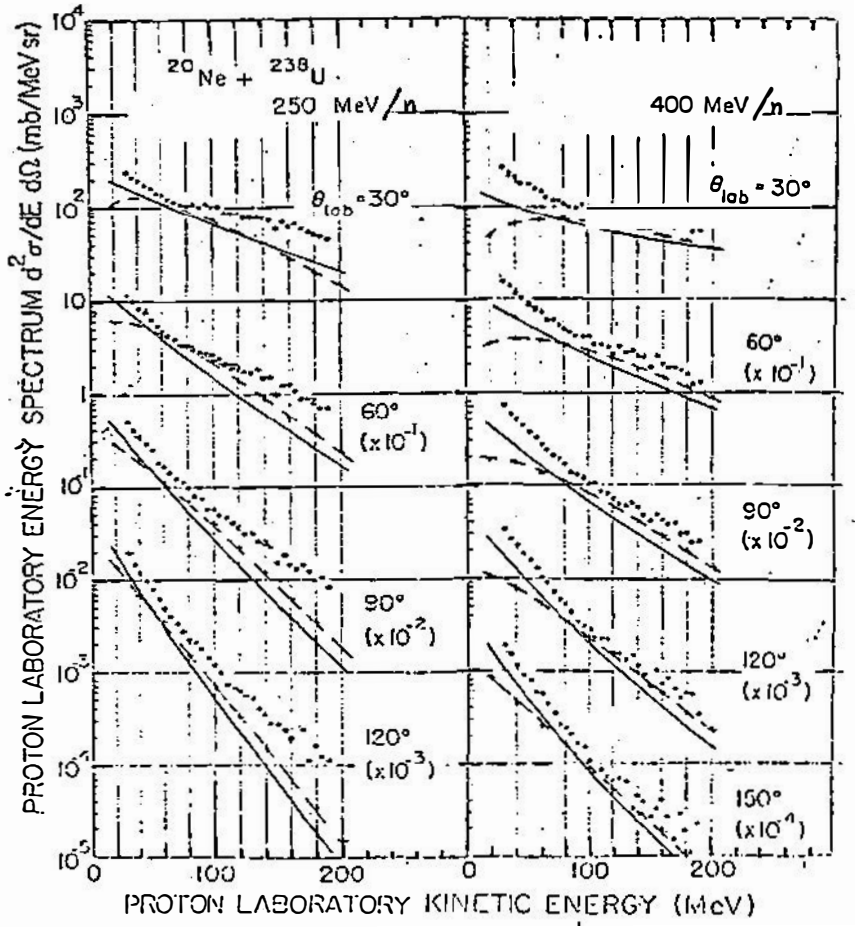

Fig. 7. Proton inclusive cross sections for Ne + U at 250 and 400 MeV/nuc. Solid curves correspond to the Firestreak model, and dashed lines correspond to Fireball model. Coalescence corrected data[11] are indicated by dots. (Fig. 6, Ref. (12)).

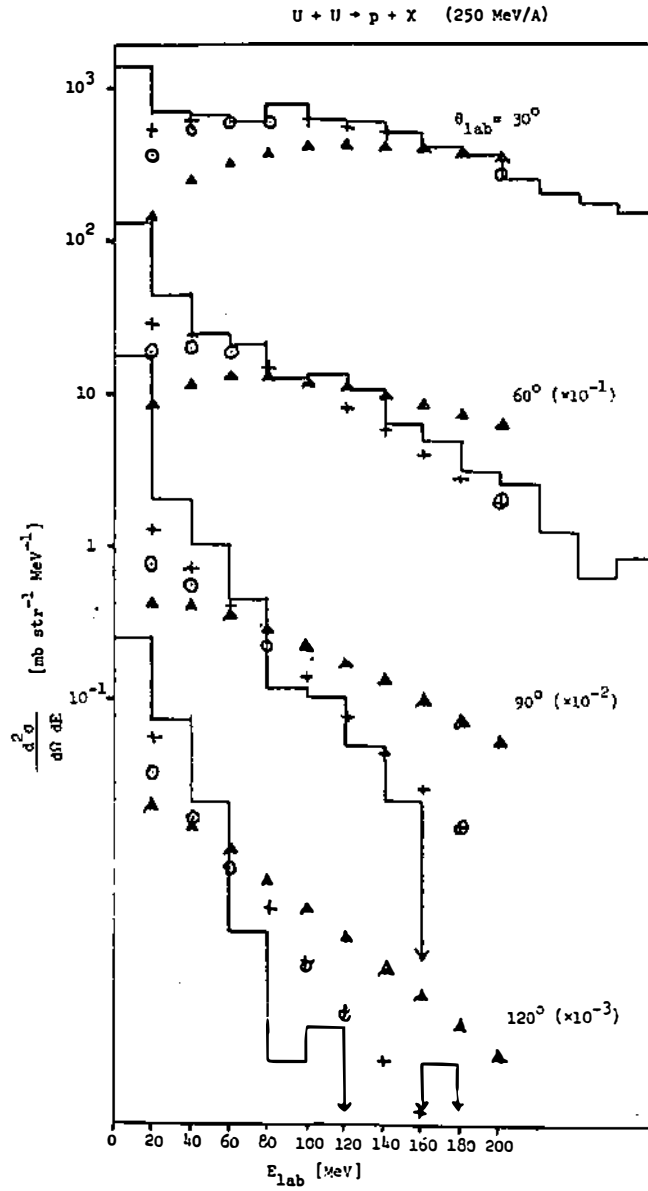

Fig. 8. Preliminary results[29] of 2-fluids (histogram), Fireball (Δ points), Firestreak (with + and without θ diffuseness) models for U + U → p + X at 250 MeV/nucl.

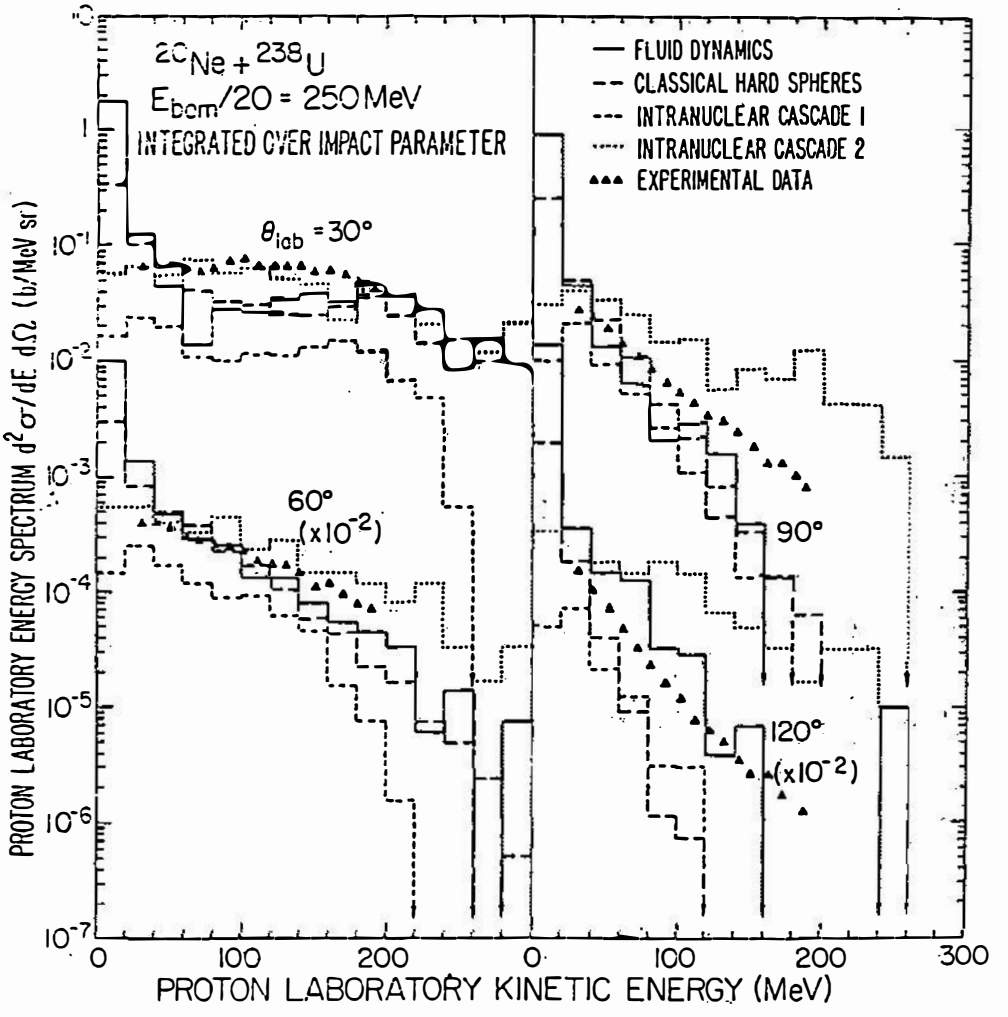

Fig. 9. Proton inclusive cross sections for Ne + U at 250 MeV/nuc compared to data[11] that are uncorrected for coalesced nucleons. Five of the indicated models are compared. (Fig. 1, Ref. (13)).

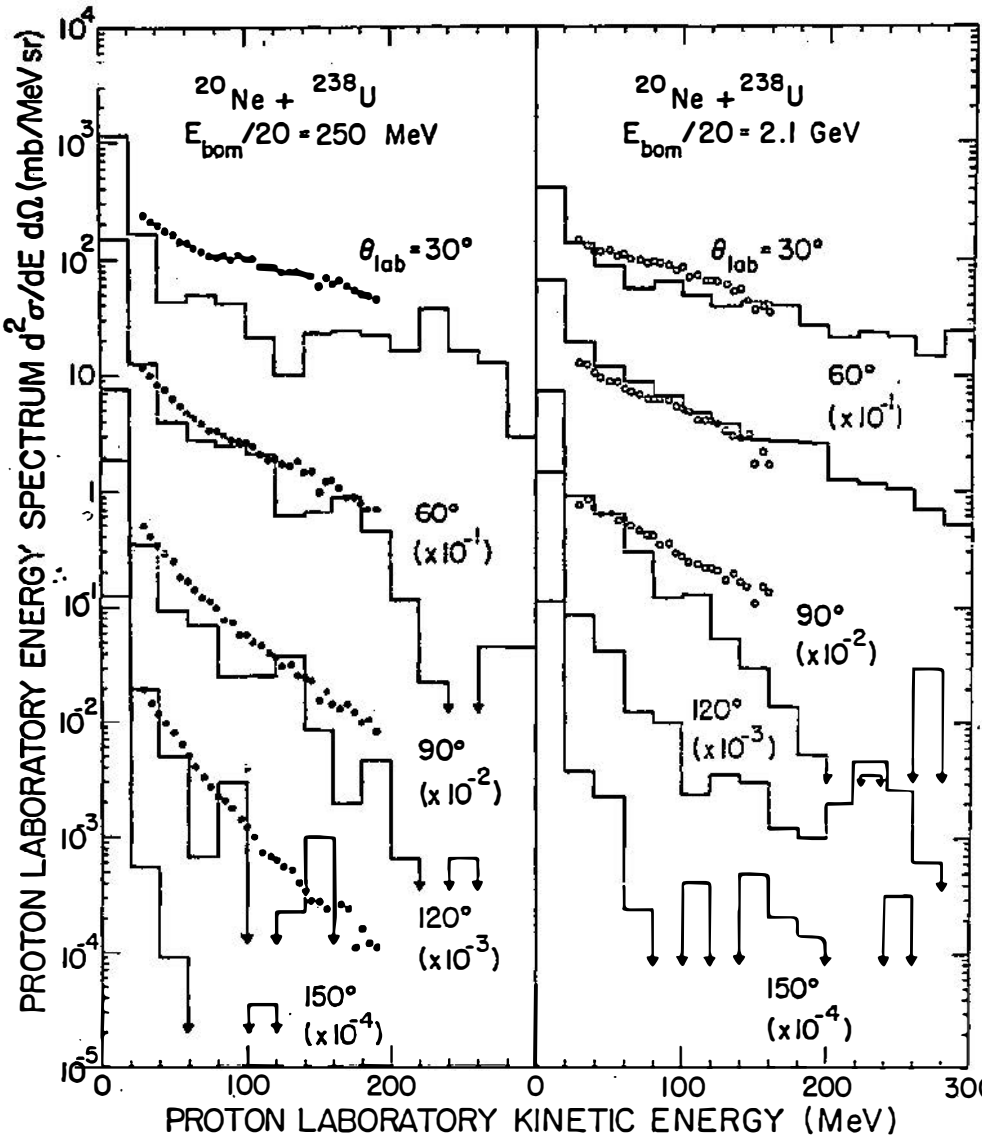

Fig. 10. Results of 2-fluids model[24] (histogram) compared to coalescence corrected data[11] (dots).

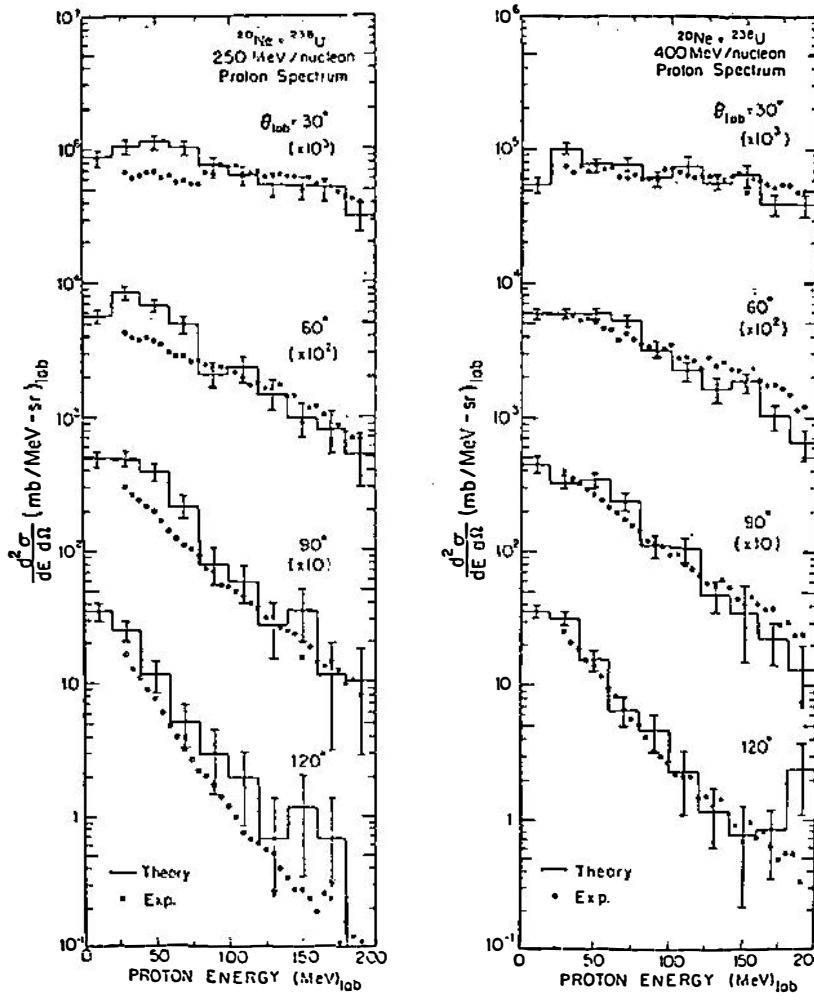

Fig. 11. Results of Cascade 2 (histogram) for Ne + U → p + X compared to uncorrected data. (Fig. 1, Ref. (16)).

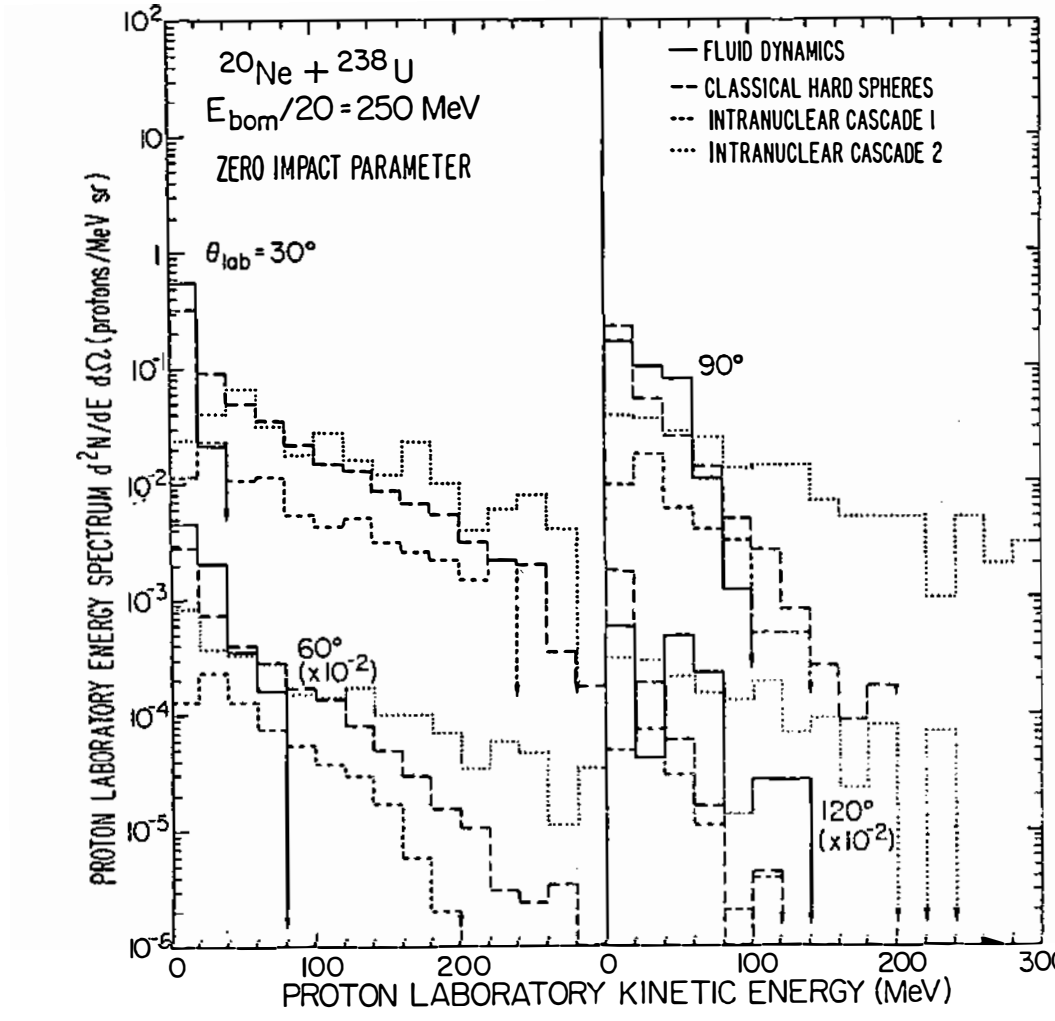

Fig. 12. Same as Fig. 9 but for zero impact parameter only. (Fig. 3, Ref. (13)).

DISCUSSION

J.J. Griffin: 1) How much parametric freedom is available to the theorist in these cascade calculations?
2) Could you elaborate your comment that $A_1=A_2$ collisions are optimal for learning about zero impact parameter collisions?

M. Gyulassy: 1) There are no explicit free parameters in the cascade calculations since experimental NN cross sections are used as input. However, there are plenty of prescriptions on the way binding, density depletion, etc. are treated. Variations of these prescriptions can result in large variations in the final results. Also numerical parameters such as the time step size effect considerably the final results.
2) The main reason for concentrating on equal mass projectile, target combinations in the future is to optimize the experimental possibility of devising a $b\approx 0$ trigger as discussed in the proceedings. For asymmetric combinations the absence of fast forward fragments can occur within a large range of impact parameters. For symmetric systems, as soon as $b\gtrsim 1$ fm the projectile and target cease to overlap and the projectile cap will result in fast forward fragments. Also azimuthal asymmetry for A+A systems will be much stronger for $b\gtrsim 1$ fm than for $A_p < A_T$.

N. Cindro: I greatly enyojed your talk, since I understood it, which means that the models are really very simple. What struck me, is the fact that none of these models made reference to nuclear structure and yet yielded resonable results. While this on one hand is nice, it also may mean that we do not need nuclear structure to explain the heavy ion data or, that, in other words, nuclear structure information is washed out in this energy domain.

M. Gyulassy: Because of the very high excitation energies ($E^*\sim(50\text{-}100)$ MeV/A) at these beam energies, nuclear structure effects are indeed washed out. Nevertheless, the dynamic does depend on the bulk properties of nuclear matter via the equation of state $W(\rho,T)$. At high energies, we would like to de-

termine $W(\rho,T)$ and leave nuclear structure studies to the low energies.

The success of the different models in reproducing data was shown to be due to a large extent to the impact parameter summation implicit in the data. In the future when $b \approx 0$ data on A+A collisions will be available, I believe the models will give rather different results.

J. Németh: Do you know any calculation in which the compressibility was determined for high temperature? From astrophysical avidence we know that the matter at $\rho \sim 5\text{-}10\,\rho_0$ is very stiff at zero temperature. How does this change at high excitation energy?

M. Gyulassy: So far only b summed data has been available which is completely insensitive to $W(\rho,T)$ and in particular to K. When $b \approx 0$ collisions will be measured, there is hope that at least the qualitative magnitude of K could be determined. At present nothing is known about $W(\rho,T)$ at high temperatures. In the hydrodynamic model the temperature dependence of $W(\rho,T)$ is assumed to be of the form of the ideal Fermi gas. This of course may have nothing to do with reality. In particular, the assumption that W can be written as a sum of a compression energy $W_{comp}(\rho)$ and a thermal energy $W_{th}(\rho,T)$ is highly questionable.